

CONSTRUCTION AND BEAM COMMISSIONING OF THE GeV-RANGE TEST BEAMLINE AT KEK PF-AR

C. Mitsuda*, T. Honda, S. Nagahashi, D. Naito, T. Nogami, N. Nakamura, H. Sasaki, S. Sakanaka,
H. Takaki, T. Uchiyama, N. Yamamoto, T. Mori, K. Satoh, KEK Accelerator Laboratory
K. Hanagaki, Y. Ikegami, I. Nakamura, M. Togawa, KEK Institute of Particle and Nuclear Studies
S. Abe, J. Maeda, N. Teramura, Kobe University
A. Maeda, K. Sumi, Nagoya University, T. Odagawa, Kyoto University

Abstract

Commissioning a test beamline in KEK Photon Factory Advanced Ring (PF-AR), which is operated by the energy of 6.5 GeV and 5.0 GeV, is proceeded in cooperation with the KEK Institute for Particle and Nuclear Studies (IPNS) to use electron beams in the GeV-range for the development of detectors in particle physics experiments. The electron can be obtained from gamma rays emitted by collisions between the halo of a stored electron beam in PF-AR, and a wire target using a copper converter to electron-positron pair creation. A yielded monochromatic electron beam is guided to the test area by quadrupole magnets and a bending magnet on the test beamline. The trial of long-user operation with top-up injection was completed in the fall of 2022.

INTRODUCTION

The history of the test beamline in KEK goes back to the construction of the Fuji Test Beam Line (FTBL) in the KEKB ring which was the first and authentic test beamline in KEK in 2007 [1, 2]. However, the FTBL was not operated as a user machine because the electron yield was not sufficiently acquired in the use of the collision between the electron and the residual gas in the vacuum duct. Although the plan to adopt the measure to use the wire target (WT) for the stored beam in the PF-AR remained out of consideration for a long time since 2014, the plan was advanced starting with budgeting in FY2020, and concrete design, fabrication, and procurement of equipment proceeded at a rapid pace during FY2020, with construction completed in the summer of FY2021.

PREPARATIONS FOR CONSTRUCTION

The test beamline stage is separated from the PF-AR ring area by a concrete radiation shield (see Fig. 1); since the irradiation tests of the electron beam are conducted on the stage side, it is necessary to transport the electron beam produced in the PF-AR ring to the stage side. The electron beam is transported to the stage area by a simple optics of transport line including a bending magnet to produce a monochromatic electron beam. The transport line is called an AR test beamline (AR-TBL) [3]. The transport line has no vacuum duct: the electron beam passes in the air. The beta function and beam emittance are 20.6 m and 290 nmrad at the WT place in the PF-AR. When WT is inserted at 5.4σ,

which is 10.8 mm and 14 mm for the stored electron energy of a 5.0 GeV and a 6.5 GeV respectively, from the beam center, assuming $\phi 0.1$ mm carbon fiber, 2.5×10^9 electrons per second collide with WT and the photons are generated in the energy spread with cut-off energy of stored electron energy.

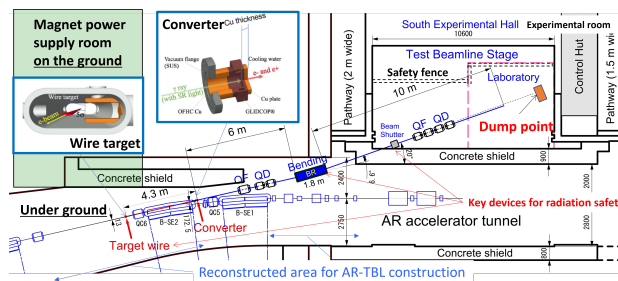


Figure 1: Schematic view of AR-TBL.

The position of the WT is finely tuned so that the electron loss due to collisions with the target is equivalent to the loss rate (6.5×10^6 photons/s) corresponding to the lifetime of an electron beam current of 20 h. This definition was decided by the energy acceptance of $\Delta p/p = 0.9\%$ in the PF-AR and the electron rate of 0.26% which has an energy loss out of its acceptance. The loss rate depends on the material of the target wire as called its the collision cross section, so the adjustment is made by measuring the actual beam lifetime precisely. The WT system is established to introduce the two wire targets separately. This measure can ensure continuous operation even when one wire target is broken accidentally. Both carbon nanotube (CNT yarns) and graphene sheets were installed for the target wire in the first beam commissioning to confirm the reliability for the operation. CNT yarns have a thermal conductivity lower than that of graphene sheets, but since the collision cross-section is larger than that of the graphene sheets, the electron yields larger than the graphene sheet was expected in CNT yarns. However, in the beam commissioning, because the heat generation and charging-up in CNT yarns were observed in the watch camera, the WT was finally unified as the graphene sheet.

At an electron beam energy of 5.0 GeV, the maximum conversion ratio of photons to electron beams of 1 GeV/c is about 14% when the copper converter thickness is 16 mm. The converter was installed in a newly made vacuum duct downstream of the bending magnet (B-SE2 in Fig. 1).

* chikaori.mitsuda@kek.jp

SYSTEM INSTALLATION

WT System and Converter Duct

The heat removal system of the water cooling system on the WT system was configured to deal with the heat generated by the target material irradiated by synchrotron radiation as identified through thermal analysis by using an ANSYS workbench. The impedance analysis of the WT chamber and the insertion jig of WT was conducted to mitigate the concentration of wakefield for beam wall current caused by the stored beam by using the CST wakefield solver. For the heat removal system, assuming the parameter for PF-AR operation, 6.5 GeV of electron beam energy, 0.05 A of stored beam current, and 23.708 m of electron orbital radius, the radiation power per 1 rad of orbit angle is estimated at 53.0 W as a heat source. Based on the radiation power irradiated to WT, the maximum temperature in CNT yarns and graphene sheet reaches 285 and 35 degrees respectively by using the copper jig to fix the WT in the simulation of the heat transfer analysis. The reached temperatures for the absorber and converter cooled by water were 319 degrees and 47 degrees in each case. Because the WT holder is inserted deeply into the vacuum duct at the defined position and the large aperture storing the WT holder and rod is opened for the side wall of the beam duct, in this case, resonant modes of electromagnetic fields generated in the chamber cannot be ignored. If resonant modes are created, strong wakefields may be excited, eventually causing heat generation and discharge. The power loss in the whole chamber is estimated at 26.6 W and the temperature only reaches about 40 degrees at most. It is concluded that the WT system would be operated safely in the case of adding the wakefield effect.

Figure 2(a) shows a view of the WT system installed in the PF-AR ring, where the two target materials mentioned above are driven separately by stepping motors with 1 μ m resolution and can be inserted at any position from any stored beam to survey the optimize the WT position which causes the defined rate of electron loss. Two types of ports are provided: a viewport to check wire position from the top and a viewport with a camera to check wire status from the front. During operation, the camera, which is moved out of the beamline plane to prevent radiation damage, can be used to check for wire damage in real-time.

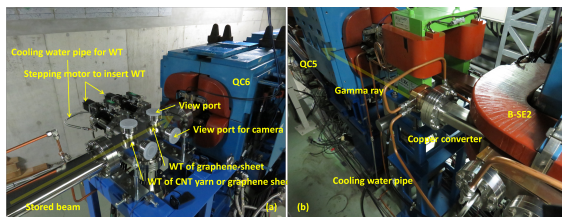


Figure 2: Wire target system.

Figure 2(b) shows the water-cooled copper converter after installation: Fig. 2(b) is a picture of the top view looking down from the outer side and upstream of the ring. The converter was installed by replacing all of the existing bend-

ing magnet (B-SE2) ducts. The transport line is close to the accelerator ring magnets. Although the magnetic field strength is measured at 10 G near the nearest B-SE1 bending magnet, it is reduced to 2 G at the position where the bending magnet (BR in Fig. 1) is installed in the AR-TBL, which is the geomagnetic level.

Magnet System in AR-TBL

The optics of the transport line consists of one QF magnet and two QD magnets with different magnet lengths for the QF and QD doublets upstream of the bending magnets, and two quadrupole magnets each for QF and QD on the downstream irradiation experiment stage as well. The assumed irradiation point is 18.3 m downstream from the converter and 3 m upstream from the dump point loaded with lead blocks; the quadrupole magnet positions were optimized so that the beam size at the irradiation point with 2 GeV/c momentum is about horizontal $1\sigma = 10$ mm and vertical $1\sigma = 2$ mm. The beam shape is such that it can be transported through the transport line without loss even if a circular duct with an inner diameter of $\phi 46$ mm is installed.

Table 1: Summary of Magnet Specification in AR-TBL

Name	Length/Bore/Gap	Field strength	Current
QRF	500/ $\phi 52$ mm	16.0 T/m	50 A
QRD1, 2	360/ $\phi 52$ mm	12.5 T/m	28 A
BR	1780/34 mm	1.2 T	200 A
QSF1, 2	360/ $\phi 52$ mm	12.5 T/m	28 A
QSD1, 2	360/ $\phi 52$ mm	12.5 T/m	28 A
V-St1, 2	250/54 mm	37.7 μ T	3 A

Table 1 shows the specifications of the magnets from the upper stream of AR-TBL. Only one bending magnet is water-cooled, and the other seven quadrupole magnets are air-cooled. The bending magnet has a horizontal correction coil wound on the back legs, and two steering magnets are added as vertical correction magnets just upstream of the QRF magnet and just downstream of the QRD2 magnet. Horizontal orbit correction is strongly dependent on the angle of collision of the stored beam on the WT and requires orbit correction by local bumping in the PF-AR ring similar to the light axis correction for the BL of the SR user. The magnets were aligned with the coordinate of the ring magnets. The alignment results are as follows: the deviation of the height level is less than 0.1 mm, the deviation of the position for the beam direction is 0.07 mm, and the deviation of the horizontal position is 0.06 mm.

The flatness of the integrated magnetic field of the bending magnet is 1×10^{-4} in the horizontal region of ± 25 mm at the medium plane of the magnet. An integrated magnetic field of 2.21 Tm can be obtained at a rated current of 200 A in the magnet central. When selecting the 2.0 GeV of an electron beam energy observed in the stage of AR-TBL, its kick angle is set to $K_0 = 115$ mrad by a current of 69 A. The quadrupole magnets can be unified because their bore

diameters are the same. The 4.74 T (B'L) is obtained for 30 A of current. For the observation of the 2.0 GeV electron beam energy on the stage, their kick angles are tuned to 0.53, -0.278, 0.275, and 0.258 mrad respectively at a current of 16.6 A. The focused beam is observed at the size of $\sigma_x = 15$ mm and $\sigma_y = 4$ mm finally at the irradiation point.

All power supplies of magnets are air-cooled. Since the BR power supply plays a key role in the energy selection of the electron beam, the stability of the power supply is compensated with a level (55 ppm) that is one order of magnitude below the required energy resolution. Compact and relatively inexpensive catalog power supplies were selected for the quadrupole and dipole correction magnet (model numbers, HX-S-060-100G and BWS40-7.5, respectively) to minimize construction costs. Each output cable of a negative line is clamped to a CAEN DCCT to precisely monitor current values during the irradiation test on the stage.

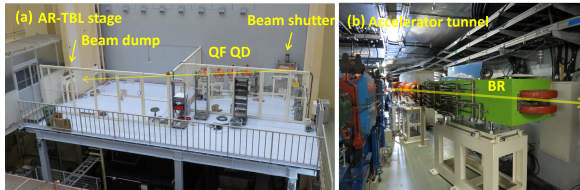


Figure 3: Completed AR-TBL.

Beam Shutter System and Beam Dump in AR-TBL

Figure 3 shows the completed AR-TBL. The beam shutter system and the beam dump are the key components of the system to ensure the safety of the experiment on the stage shown in Fig. 3(a). The beam shutter's open/close state is incorporated as a condition for the safety interlock system separated from the accelerator operation. When the main beam shutter is closed, the user can freely enter and exit the experimental area. However, if the fence door is opened while the main beam shutter is open to use the electron beam, that is, if someone enters the area (in case of an anomaly), the main beam shutter is immediately closed, the power supply of bending magnet (Fig. 3(b)) is turned off, and the target is pulled out from the stored beam position. As a precaution, but assuming a worst-case scenario, these three requirements were not met, the stored beam is dumped by the accelerator interlock system. The beam shutter can be opened only when the TBL shutter permit is given to the AR-TBL experimental stage by the accelerator operator. A SUS pipe with an inner diameter of $\phi 56.5$ mm was passed through the hole penetrated in the concrete wall of the PF-AR accelerator ring, and the surrounding gap between the SUS pipe and concrete wall was filled with lead (Fig. 3(a)). The shielding effect was estimated to be more than 900 mm thick in terms of concrete. The electron beams not selected by the bending magnets are shielded by the concrete wall and lead. The shutters are made of steel with a thickness of 30 cm. The beam dump point is located in front of the control hut on the stage and consists of lead blocks, which whole size is 200 mm thick and 250 mm wide, and an electromagnetic

calorimeter composed of a PMT and a lead glass counter for measuring the electron energy.

BEAM COMMISSIONING

In the fall of 2021, the WT was inserted into the position where a loss rate of the expected beam lifetime of $\tau = 20$ h was observed while watching the baking effect of the collision with the WT monitoring the deterioration of a vacuum value. The changing point in beam lifetime was roughly confirmed by inserting in 1 mm steps, and the exact beam lifetime boundary point exists in a narrow range of 0.1 mm steps and 1 mm depth widths.

In the practical beam commissioning, the COD of about 40 μm was found to be generated by the excitation of three quadrupole magnets and bending magnets. The COD correction program real-timely compensated the orbit distortion in the storage ring, and no light axis distortion in the SR beamline side was caused. A full-scale collision experiment in which the WT was placed at the defined position with a long run of 8 h of continuous electron-beam transportation to the AR-TBL stage was first succeeded in the stored beam mode in 2022. The WT was monitored by a scintillation counter at the AR-TBL stage using the WT of the graphene sheet, and a survey was performed in steps of 0.1 mm from the center of the stored beam position (Fig. 4(a)). A stable rate of electrons of 1000 count/s was observed at a 14.3 mm position. Both the position of the WT and the energy distribution of the electron beam (Fig. 4(b)) which are shown in Fig. 4 met the expectations and requirements. Following the above successes, we confirmed the long-term durability of the WT that accidental discharge damage did not occur while the injected and stored beams constantly collided with the WT, and that the beam loss by the WT was constantly kept while the stored beam current was maintained by the top-up injection even if the horizontally stored-beam oscillation was caused by the top-up injection. The AR-TBL user operation is planned to start in FY2023.

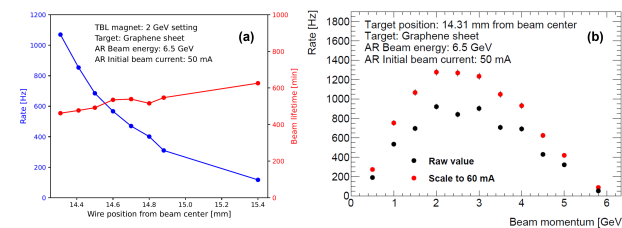


Figure 4: Distributions of electron yield observed on the AR-TBL stage.

ACKNOWLEDGEMENTS

We would like to thank the members of KEK IPNS, KEK IMSS and KEK ACCL for their cooperation in arranging the budget, the modification of PF-AR ring, and the commissioning time of machine study.

REFERENCES

[1] J. Haba *et al.*, *Journal of the Particle Accelerator Society of Japan, Accelerator*, vol. 4, no. 2, pp. 131–135, 2007. (in Japanese)

[2] T. Egawa *et al.*, *Journal of the Particle Accelerator Society of Japan, Accelerator*, vol. 4, no. 4, pp. 318–325, 2007. (in Japanese)

[3] T. Honda *et al.*, in *Proceedings of the 18th Annual Meeting of Particle Accelerator Society of Japan, QST-Takasaki Online*, Japan, Aug. 2021, pp. 379–383. (in Japanese)